Deconvoluting ultrafast structural dynamics: temporal resolution beyond the pulse length of synchrotron radiation

Richard Neutze* and Remco Wouts

Department of Biochemistry, Biomedical Centre, Uppsala University, Box 576, S-75123 Uppsala, Sweden. E-mail: neutze@xray.bmc.uu.se

100 picosecond X-ray snapshots visualizing the structural dynamics of macromolecular systems are now routinely available at synchrotron sources. A wealth of fundamental processes in photochemistry, condensed matter physics and biology, however, occur on considerably faster time scales. Standard experimental protocols at synchrotron sources cannot provide structural information with faster temporal resolution as these are limited by the duration of the electron bunch within the synchrotron ring. By walking the timing of femtosecond laser photolysis through a (much longer) X-ray pulse in steps of a few picoseconds, structural information on ultrafast dynamics may be retrieved from a set of X-ray scattering images, initially through deconvolution and subsequently through refinement. This experimental protocol promises immediate improvements in the temporal resolution available at synchrotron sources, facilitating the study of a number of rapid complex photochemical processes. Combined with techniques which reshape the X-ray probe pulse, the accessible temporal domain could further be extended to near-picosecond resolution.

Keywords: time-resolved X-ray crystallography; structural dynamics.

1. Current technology

Experimental development of techniques in picosecond/ femtosecond laser spectroscopy have opened powerful windows onto a wealth of photochemical processes which lie in the ultrafast temporal domain. Alkene photo-isomerization both within solution (Courtney & Fleming, 1983) and within a protein (Gia *et al.*, 1998); the environment's influence on the chemical dynamics of photo-dissociation and geminate recombination of molecules in solution (Harris *et al.*, 1987); the photodetachment of ligands from ligand-binding haem proteins (Franzen *et al.*, 1995); structural phase transitions within crystals (Dougherty *et al.*, 1992); or the rapid transfer of heat to a semiconductor lattice (Tom *et al.*, 1988), list but a few of the systems for which ultrafast spectroscopy studies have provided an empirical basis for theoretical modelling.

All these phenomena invariably induce specific structural rearrangements of both the chromophore of interest and the surrounding environment. While spectroscopic techniques probe the electronic and vibrational transitions of the photoactivated sample, any structural rearrangements must be inferred from spectroscopic observations and therefore require a detailed theoretical understanding of the energy surfaces of the excited system. X-ray scattering and diffraction techniques, in contrast, provide a direct probe of the geometry of molecules at atomic resolution. An extension of existing time-resolved X-ray diffraction techniques into the ultrafast regime, in combi-

nation with femtosecond laser photolysis, would undoubtedly yield new understanding of the most rapid structural changes.

Momentum towards picosecond/subpicosecond structural studies has been provided by a number of techniques: Rischel *et al.* (1997) used a pulsed laser plasma X-ray source to track the heating of an organic film; Schoenlein *et al.* (1996) used 90° Thompson scattering from a relativistic electron bunch to shift the frequency of a femtosecond laser pulse into the X-ray realm; Zholents & Zolotorev (1996) have proposed other schemes for interacting a femtosecond light pulse with an electron bunch; Larsson *et al.* (1998) melted two X-ray mirrors in rapid succession and the recorded X-ray intensities were correlated with their relative delay. All successful experiments to date, however, share one feature in common: all recorded X-ray scattering from a single diffraction spot. High-temporal-resolution detectors, such as X-ray streak cameras (Shepherd *et al.*, 1995), are also intrinsically one-dimensional in nature and suffer from a low quantum efficiency ($\sim$1%). Near-picosecond-resolution studies have also been performed using electron scattering from photodissociated molecules within a molecular beam (Williamson *et al.*, 1997). The extremely high cross sections of electrons relative to X-rays, however, cause insurmountable problems should one wish to move away from a vacuum sample environment.

It is therefore apparent that if three-dimensional structural information is desired from more complicated systems such as macromolecules, inorganic crystals with medium

unit-cell dimensions, or diffuse scattering from photo-chemical systems in solution, techniques which utilize the brightest available light sources and which are compatible with existing two-dimensional X-ray detectors are required. Synchrotron radiation provides the most brilliant source of X-rays available within current technology. Its application to time-resolved macromolecular crystallography yields excellent-quality diffraction data, with a number of atomic resolution structures of protein reaction intermediates having been reported (*e.g.* Williams *et al.*, 1997; Genick *et al.*, 1998; Käck *et al.*, 1998). A drive towards visualizing extremely rapid structural dynamics has isolated 100 ps X-ray pulses from an individual electron bunch within the synchrotron ring, from which Srajer *et al.* (1996) and Perman *et al.* (1998) have recorded interpretable Laue (white X-ray beam) diffraction images from short-lived protein photointermediates.

In spite of the current availability of femtosecond laser facilities online at synchrotron sources (Schoenlein *et al.*, 1996; Wulff *et al.*, 1997; Larsson *et al.*, 1998), standard experimental protocols are limited in their temporal resolution by the duration of the X-ray pulse (~100 ps), too slow to visualize the transient dynamics of most of those processes listed above. In this article we describe a theoretical basis for analysing synchrotron-based pump–probe experiments with two-dimensional detectors. This leads us to propose a scheme of combined deconvolution and refinement which would push the temporal resolution beyond current limitations. By providing a methodology which enables X-ray scattering to be recorded on two-dimensional X-ray detectors, a broad range of problems become accessible on the ultrafast time scale which cannot be approached using the successful one-dimensional pico-second-resolution X-ray methodologies reported to date (Rischel *et al.*, 1997; Larsson *et al.*, 1998).

2. Deconvolution protocol

Suppose any photoactive sample (*i.e.* not necessarily crystalline) is exposed to an X-ray pulse with a time-dependent intensity $P(t)$. Typically, single-bunch pulses at a synchrotron source have a duration $T \simeq 100$ ps. Define t_i as the time delay between the arrival of the X-ray (probe) pulse peak ($t = 0$) relative to sample triggering by a femtosecond laser pulse. As laser photolysis can be achieved more than an order of magnitude faster than the time resolution discussed here, it is sufficient to treat photoactivation as instantaneous. This differs from a standard pump–probe spectroscopy experiment, where both pump and probe light pulses are typically of a similar duration. Following photoactivation the sample may be described by a time-dependent electron density $\rho(t + t_i)$ with density peaks centred at the atomic positions $\mathbf{x}_j(t + t_i)$. X-ray scattering factors for the photoactivated sample at time t are therefore

$$F_{\mathbf{h}}(t + t_i) \equiv \sum_j f_j \exp\left[i\,(2\pi/\lambda)\mathbf{h} \cdot \mathbf{x}_j(t + t_i)\right], \qquad (1)$$

where j ranges over all atoms in the sample; for all $\tau \leq 0$, $F_{\mathbf{h}}(\tau) = F_{\mathbf{h}}^0$ represents scattering from the unexcited sample; we have absorbed all constant scaling coefficients (*e.g.* r_e^2 and X-ray polarization factors) in our definition of the atomic scattering factors f_j; and $\mathbf{h}$ lies in reciprocal space. For crystalline samples the components of $\mathbf{h}$ (expressed relative to the crystal's reciprocal lattice) take only integer values, whereas scattering from amorphous substances produces a continuous scattering distribution (James, 1948). Had the X-ray and laser pulses been of similar duration, an additional integral over the laser pulse profile would have been required in equation (1), considerably complicating the extraction of useful data in any experiment.

At each instant the X-ray scattering intensity is proportional to the product of the X-ray pulse intensity, $P(t)$, with $|F_{\mathbf{h}}(t + t_i)|^2$. A standard two-dimensional X-ray detector without time resolution (*e.g.* a CCD) integrates the instantaneous scattering intensity (each pixel of the detector mapping to a vector in reciprocal space) over time, such that (Neutze & Hajdu, 1997)

$$I_{\mathbf{h}}(t_i) = \int_{-\infty}^{\infty} P(t)\,\left|F_{\mathbf{h}}(t + t_i)\right|^2 \,\mathrm{d}t, \qquad (2)$$

with every recorded image containing information on the structural dynamics of the system over a time domain defined by the X-ray pulse duration. By recording X-ray scattering images with one specific time delay t_i, the standard experimental protocol, one cannot recover dynamical information on a faster time scale. Upon the substitution $t \to u = -t$ and writing the temporal profile of the X-ray pulse as a sum of its symmetric and antisymmetric components, however, equation (2) may be recognized as a convolution,

$$I_{\mathbf{h}}(t_i) = \int_{-\infty}^{\infty} \left[P_s(u) - P_a(u)\right]\left|F_{\mathbf{h}}(t_i - u)\right|^2 \,\mathrm{d}u$$

$$\equiv \left[P_s(t_i) - P_a(t_i)\right] \otimes \left|F_{\mathbf{h}}(t_i)\right|^2. \qquad (3)$$

This suggests that, with appropriate sampling, the temporal profile of the X-ray probe pulse can be deconvolved.

An experimental protocol would be to collect a series of X-ray scattering images $I_{\mathbf{h}}(t_i)$, $i = 1$ to N, for which the delay of the X-ray pulse peak, t_i, relative to the moment of sample photolysis is walked, in steps of duration $\Delta t \ll T$, entirely through $P(t)$: from the photoexcitation pulse arriving at time T following the X-ray pulse's maximum (so that essentially no photoactivation is caught in the X-ray image); arriving simultaneously with the peak in the X-ray pulse (when the maximum contribution from the initially photoactivated sample can be expected); to arriving at time T in advance of the X-ray peak (the entire X-ray pulse thereby yielding information on processes following photoactivation). For one complete experiment, $N > T/\Delta t$ images would need to be recorded, and the entire data set

can initially be deconvoluted and subsequently refined so as to obtain significant improvements in the temporal resolution available at synchrotron sources.

The deconvolution problem is well known and has been studied extensively. Ideally one could recover $|F_{\mathbf{h}}(t_i)|^2$ for each time point directly by taking the Fourier transform of equation (3), dividing through by $\mathcal{F}\left[P_s(t_i) - P_a(t_i)\right] = P^*(\Omega)$ (* denotes complex conjugate), and evaluating the inverse Fourier transform. In practice, however, significant limitations usually apply. In this case a number of intrinsic advantages arise which will assist the analysis of experimental data. By recording X-ray scattering on a two-dimensional detector, literally thousands of correlated observations are made simultaneously. This redundancy enables minimization algorithms to be utilized which decreases the sensitivity to errors in any one measurement. The time scales of the system of study can be characterized through ultrafast spectroscopy, and this additional information should be incorporated within algorithms refining (with time as an additional variable) the structural dynamics of the system. In contrast to optical pump–probe experiments, photoexcitation is effectively instantaneous which side-steps the problem of an additional convolution with the pump profile. Furthermore, the X-ray source itself is unusually stable and the pulse shape is asymmetric when the current is large. As such, the spectral domain of the pulse contains stronger high-frequency components which increases confidence in the deconvolution results. These factors combined make it likely that interpretable scattering-factor amplitudes can be retrieved after deconvolution.

3. Experimental considerations

Two features of this methodology should be appreciated: the technological infrastructure required for such experiments is now available at synchrotron sources (Wulff *et al.*, 1997; Larsson *et al.*, 1998); and numerical deconvolution may be implemented with standard algorithms (*e.g.* Press *et al.*, 1988). The success of any such experiment, however, is very dependent on the parameters of the synchrotron source, synchronization electronics and detector efficiency. Experiments performed at the Advanced Light Source (ALS) and the European Synchrotron Radiation Facility (ESRF) provide suitable comparisons with which to judge the potential of a deconvolution approach. Current technical developments at other third-generation synchrotron facilities shall also make available dedicated beamlines for time-resolved experiments.

X-ray flux requirements and detector technology have been proven experimentally, with Srajer *et al.* (1996) having recorded interpretable Laue diffraction images from crystals of myoglobin upon integrating only three 100 ps X-ray pulses prior to reading the low-noise CCD detector. With stroboscopic data-collection techniques facilitating photoexcitation and X-ray exposure cycling rates of $\sim$1 kHz (Wulff *et al.*, 1997), the photon flux and detector performance available at the ESRF will certainly enable X-ray scattering images to be interpreted from a wide variety of reversible photosystems.

Electronic jitter in the firing of the femtosecond laser relative to the X-ray pulse is typically $\sim$3 ps. This causes a broadening of the X-ray pulse's temporal profile by a few percent when averaging over a large number of exposures. Measurements of the X-ray pulse's temporal profile using streak cameras have been performed at both the ALS (Larsson *et al.*, 1997) and the ESRF (Scheidt & Naylor, 1998). As femtosecond laser pulses were used to trigger these cameras, the resulting profiles already contain broadening due to electronic jitter. Provided a sufficiently large number of X-ray exposures are averaged prior to reading the X-ray detector, there is no reason to expect that jitter will pose any greater limitation in a deconvolution approach than it does in streak camera measurements.

Ultrafast experiments performed to date have isolated X-ray pulses generated by the same electron bunch within the storage ring, either through using a chopper (Wulff *et al.*, 1997) or electronically (Larsson *et al.*, 1998). Even so, resonances and instabilities can cause small variations of the pulse shape on a short time scale, and verification of the stability of the pulse shape over longer periods of time (*e.g.* through streak camera measurements) is necessary. At the ESRF the full width at half-maximum of the X-ray single bunch becomes longer as the synchrotron current is increased (Wulff *et al.*, 1997), and streak camera measurements have shown that when the current is high the X-ray pulse profile is not symmetric but rises considerably more rapidly than it falls (Scheidt & Naylor, 1998). Fig. 1(*a*) shows an approximate X-ray pulse profile which was used to simulate the potential of this deconvolution approach. At the ESRF the monochromatic X-ray flux is $\geq 10^6$ photons per pulse, which was averaged over 100 pulses in generating Fig. 1(*a*).

As an example, suppose that the maximum change in X-ray scattering intensity from a photoactivated sample occurs immediately after photolysis and then decays exponentially. Using equation (2) to predict the measured intensity, taking the intrinsic experimental noise of any measurement as a Gaussian distribution with σ being 5% of $\Delta I_{\max}$, and applying a frequency filter prior to deconvolution, yields the predictions of Figs. 1(*b*) and 1(*c*). Each figure shows numerical predictions obtained both through a deconvolution analysis (solid line) and assuming an idealized measurement (dashed line) for which a hypothetical X-ray probe of infinitesimal duration is used. The time scales for these exponential decays are $\tau = 90$ ps and $\tau = 30$ ps, respectively. At this level of noise the deconvolution results shown in Figs. 1(*b*) and 1(*c*) are quite tolerant of errors of a few percent in the X-ray pulse profile.

All observed time scales may be corroborated *via* picosecond spectroscopy or, in turn, picosecond spectroscopy results may be used to aid the extraction of dynamical structural data. From a knowledge of the initial structure and phases for the unperturbed sample, $F_{\mathbf{h}}^0$, difference

electron density maps can be calculated for each time point t_i, providing a first estimate for the time-dependent atomic positions of the photoexcited sample, $\mathbf{x}_j(-t_i)$. Refinement
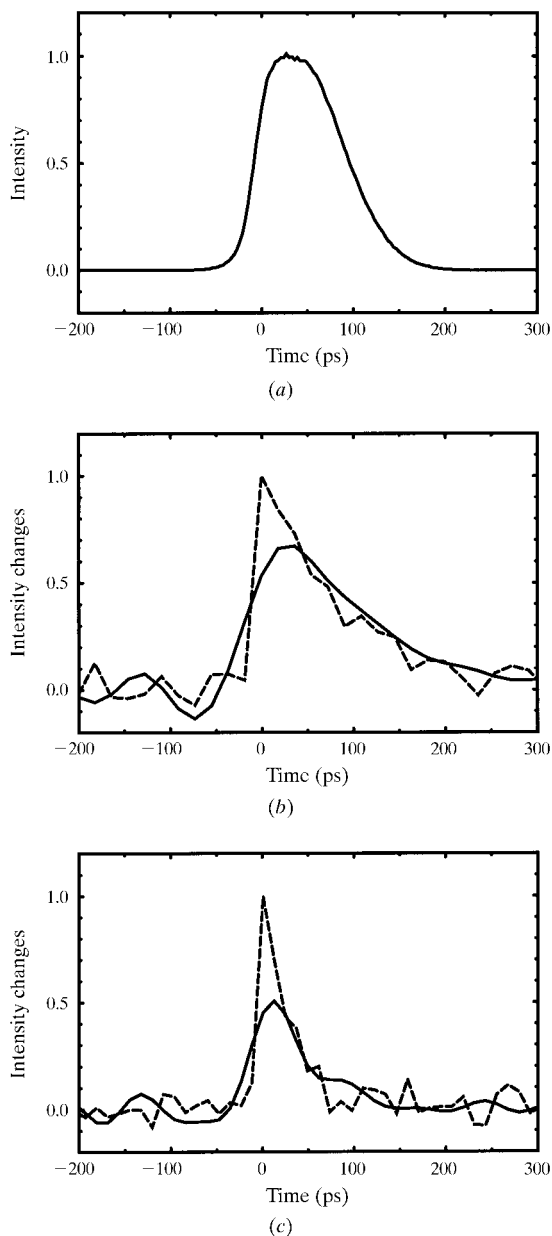

(a)

(b)

(c)

Figure 1
Illustration of a deconvolution approach using a realistic X-ray pulse profile. (a) The X-ray pulse profile used for these simulations, which approximates the measured single-bunch pulse profile of the ESRF (courtesy of K. Scheidt and G. Naylor). (b) A comparison between the measurement of an exponential decay, $\Delta I(t) \propto \exp(-t/\tau)$, after deconvolution (solid line) with an idealized measurement (dashed line). Experimental noise was taken to obey a Gaussian distribution with standard deviation σ = 5% of ΔI_{max}, 100 steps of Δt = 18 ps were taken, and the deconvoluted signal was numerically filtered. (c) A comparison between two further simulations with the decay constant τ = 30 ps, where 100 steps of Δt = 12 ps were taken. Deconvoluted intensities as a function of time, in combination with a spectroscopic characterization of the time scales of interest, would provide a starting point from which to build and refine the sample's rapid structural dynamics. Intensity units are arbitrary.

algorithms would then proceed by simultaneously minimizing $|I_{\mathbf{h}}^{calc}(t_i)^{1/2} - I_{\mathbf{h}}^{obs}(t_i)^{1/2}|$ for all N time points t_i, combining equations (1) and (2) to calculate $I_{\mathbf{h}}^{calc}(t_i)$ from the modelled atomic positions $\mathbf{x}_j(-t_i)$.

A second example may be found in the form of a recent experiment performed at the ALS. Larsson et al. (1998) examined the rapid transfer of heat to crystals of InSb following femtosecond laser photolysis. The timing of the femtosecond laser relative to their X-ray pulse was changed in steps of $\sim$30 ps, and the intensity of a single Bragg scattering spot was recorded. On this time scale the X-ray scattering factor for this single spot could be approximated by a step function, $H(t)$. Substituting $|F(t + t_i)|^2 = H(t + t_i)$ into equation (2) and differentiating with respect to t_i [note $dH(t + t_i)/dt_i = \delta(t + t_i)$], then integrating with respect to t, gives

$$\frac{dI_{\mathbf{h}}(t_i)}{dt_i} = P(t_i),$$

which reproduces their experimental result, as Larsson et al. (1998) obtained the ALS X-ray pulse profile when differentiating their experimental intensities with respect to the laser timing. This provides experimental proof of the basic theoretical framework presented here.

Larsson et al. (1998) then extended the recovered temporal resolution by melting two crystals in succession. The principle benefit of their protocol has a simple interpretation within our analysis. By melting of the first crystal, a rapidly falling edge was induced in the temporal profile of the scattered X-ray pulse, thereby extending its domain in frequency space. This scattered pulse was then used as the probe X-ray pulse for the second crystal, thereby strengthening the higher-frequency components of the (reshaped) X-ray probe, $P(\Omega)$, making it possible to resolve rapid dynamical events with greater confidence. While Larsson et al. (1998) did not describe their experiment in terms of a deconvolution analysis, an extension of their approximately 2 ps resolution experiment to more complicated systems could very naturally be achieved by replacing their second crystal with an arbitrary sample and recording the scattered X-rays on a two-dimensional detector as described above.

4. Conclusion

Recent technical developments make available femtosecond laser facilities online at synchrotron sources. As synchrotron radiation is by far the most brilliant X-ray source currently available, the deconvolution protocol presented here provides a methodology for probing the picosecond time-scale structural dynamics of a variety of systems which require the use of two-dimensional X-ray detectors. The photodissociation of simple molecules in solution show relaxations over a range of time scales from picoseconds to nanoseconds, which could be visualized using diffuse X-ray scattering; phase transitions in inorganic materials could be structurally probed using the

technique of powder diffraction; and, while a protein sample would almost certainly not survive a large number of complete data sets, it would be possible to record a series of temporally distinct Laue diffraction images from a single-crystal orientation, thereby extracting considerably more dynamical information than would be available from a streak camera experiment monitoring a single diffraction spot.

References

Courtney, S. H. & Fleming, G. R. (1983). *J. Chem. Phys.* **83**, 215–222.

Dougherty, T. P., Wiederrecht, G. P., Nelson, K. A., Garrett, M. H., Jensen, H. P. & Warde, C. (1992). *Science*, **258**, 770–774.

Franzen, S., Bohn, B., Poyart, C. & Martin, J.-L. (1995). *Biochemistry*, **34**, 1224–1237.

Genick, U. K., Soltis, S. M., Kuhn, P., Canestrelli, I. L. & Getzoff, E. D. (1998). *Nature (London)*, **392**, 206–209.

Gia, F., Hasson, K. C., McDonald, J. C. & Anfinrud, P. A. (1998). *Science*, **279**, 1886–1891.

Harris, A. L., Brown, J. K. & Harris, C. B. (1987). *Annu. Rev. Phys. Chem.* **39**, 341–366.

James, R. W. (1948). *The Optical Principles of the Diffraction of X-rays.* Woodbridge: Oxbow.

Käck, H., Gibson, K. J., Lindqvist, Y. & Schneider, G. (1998). *Proc. Natl Acad. Sci. USA*, **95**, 5495–5500.

Larsson, J., Chang, Z., Judd, E., Schuck, P. J., Falcone, R. W., Heimann, P. A., Padmore, H. A., Kapteyn, H. C., Bucksbaum, P. H., Murnane, M. M., Lee, R. W., Machacek, A., Wark, J. S., Liu, X. & Shan, B. (1997). *Optics Lett.* **22**, 1012–1014.

Larsson, J., Heimann, P. A., Lindenberg, A. M., Schuck, P. H., Bucksbaum, P. H., Lee, R. W., Padmore, H. A., Wark, J. S. & Falcone, R. W. (1998). *Appl. Phys.* A**66**, 587–591.

Neutze, R. & Hajdu, J. (1997). *Proc. Natl Acad. Sci. USA*, **94**, 5651–5655.

Perman, B., Srajer, V., Ren, Z., Teng, T., Pradervand, C., Ursby, T., Bourgeois, D., Schotte, F., Wulff, M., Kort, R., Hellingwerf, K. & Moffat, K. (1998). *Science*, **279**, 1946–1950.

Press, W. H., Teukolsky, S. A., Vetterling, W. T. & Flannery, B. P., (1988). *Numerical Recipes in C: The Art of Scientific Computing*, 2nd ed., ch. 12. Cambridge University Press.

Rischel, C., Rousse, A., Uschmann, I., Albouy, P.-A., Geindre, J.-P., Audebert, P., Gauthier, J.-C., Förster, E., Martin, J.-L. & Antonetti, A. (1997). *Nature (London)*, **390**, 490–492.

Scheidt, K. & Naylor, G. (1998). Unpublished.

Schoenlein, R. W., Leemans, W. P., Chin, A. H., Volfbeyn, P., Glover, T. E., Balling, P., Zolotorev, M., Kim, K.-J., Chattopadhyay, S. & Shank, C. V. (1996). *Science*, **274**, 236–238.

Shepherd, R., Booth, R., Price, D., Bowers, M., Swan, D., Bonlie, J., Young, B., Dunn, J., White, B. & Stewart, R. (1995). *Rev. Sci. Instrum.* **66**, 719–721.

Srajer, V., Teng, T., Ursby, T., Pradervand, C., Ren, Z., Adachi, S., Schildkamp, W., Bourgeois, D., Wulff, M. & Moffat, K. (1996). *Science*, **274**, 1726–1729.

Tom, H. K. W., Aumiller, G. D. & Briton-Cruz, C. H. (1988). *Phys. Rev. Lett.* **60**, 1438–1441.

Williams, P. A., Fülöp, V., Garman, E. F., Saunders, N. F. W., Ferguson, S. J. & Hajdu, J. (1997). *Nature (London)*, **389**, 406–412.

Williamson, J. C., Cao, J., Ihee, H., Frey, H. & Zewail, A. H. (1997). *Nature (London)*, **386**, 159–162.

Wulff, M., Schotte, F., Naylor, G., Bourgeois, D., Moffat, K. & Mourou, G. (1997). *Nucl. Instrum. Methods Phys. Res. A*, **398**, 69–84.

Zholents, A. A. & Zolotorev, M. S. (1996). *Phys. Rev. Lett.* **76**, 912–915.